

*Full Paper***NADPH Oxidase Isoforms and Anti-hypertensive Effects of Atorvastatin Demonstrated in Two Animal Models**

Wenhao Cui¹, Kuniharu Matsuno¹, Kazumi Iwata¹, Masakazu Ibi¹, Masato Katsuyama¹, Tomoko Kakehi¹, Mika Sasaki¹, Kanako Ikami¹, Kai Zhu¹, and Chihiro Yabe-Nishimura^{1,*}

¹Department of Pharmacology, Kyoto Prefectural University of Medicine, Kyoto 602-8566, Japan

Received May 13, 2009; Accepted August 31, 2009

Abstract. Beneficial effects of statins on cardiovascular diseases have been attributed to decreased generation of reactive oxygen species (ROS). We tested the hypothesis that atorvastatin protects against the development of hypertension by reducing levels of NADPH oxidase-derived ROS in two hypertensive animal models. Atorvastatin was given to mice chronically infused with angiotensin (Ang) II or to apolipoprotein E (ApoE)-deficient mice fed a high-fat diet. Increased mean blood pressure (MBP) demonstrated in both animal models was significantly suppressed by atorvastatin with reduced ROS production in the aorta. Treatment with atorvastatin did not alter the mRNA level of NOX1, a catalytic subunit of NADPH oxidase, but decreased the levels of other NOX isoforms, NOX2 and NOX4, in the ApoE-deficient mice fed a high-fat diet. In the Ang II-infused model treated with statin, only the NOX4 mRNA level was reduced. Membrane translocation of Rac1 was significantly reduced in the Ang II-infused mice treated with atorvastatin. Finally, atorvastatin administered to Ang II-infused mice lacking the *Nox1* gene elicited an additional decline in MBP compared to *Nox1*-deficient mice treated with vehicle. Together, these findings suggest that reduced expression and activity of the isoforms of NADPH oxidase, involving NOX1, NOX2, and possibly NOX4, mediate the anti-hypertensive effect of atorvastatin.

Keywords: angiotensin II, atorvastatin, hypertension, NADPH oxidase, reactive oxygen species

Introduction

Reactive oxygen species (ROS) were primarily known as crucial molecules in host defense. Over the last decade, ROS have been also recognized as important signaling molecules that modulate the transcription of various genes via the activation of redox-sensitive protein kinases and transcription factors (1). While ROS are generated in non-enzymatic and enzymatic reactions, NADPH oxidase was identified as a major source of ROS produced in response to stimuli (2, 3). NADPH oxidase is a multicomponent enzyme comprising the membrane-bound catalytic subunits NOX and p22phox, which associate with several cytosolic regulatory subunits (4). Recently, multiple homologs of NOX were found, among which NOX1, NOX2, and NOX4 were identified in vascular tissues. Accumulating evidence

indicates that ROS generated by NADPH oxidase take part in the development of various cardiovascular disorders such as hypertension (5), aortic dissection (6), and vascular remodeling (7).

Statins, 3-hydroxy-3-methylglutaryl coenzyme A (HMG-CoA) reductase inhibitors, have been used clinically as a cholesterol-lowering drug to treat hyperlipidemia. Evidence in support of their beneficial effects on cardiovascular diseases is steadily increasing in animal studies and clinical trials (8, 9). In a chronic angiotensin (Ang) II-infusion model and in spontaneously hypertensive rats (SHR), treatment with statins reduced cardiovascular derangements by suppressing production of ROS (10, 11). Statins also demonstrated an antioxidative effect and down-regulated the expression of NADPH oxidase subunits in cultured vascular smooth muscle cells and in transgenic TG (mRen2)27 (Ren2) rats (12, 13). These findings suggest NADPH oxidase to be a crucial target of statin therapy.

In this study, we investigated the impact of statin on vascular NADPH oxidase in two murine models

*Corresponding author. nchihiro@koto.kpu-m.ac.jp

Published online in J-STAGE on October 31, 2009 (in advance)

doi: 10.1254/jphs.09148FP

of chronic hypertension. The findings suggested that atorvastatin suppresses the development of hypertension by reducing the expression and activity of the isoforms of NADPH oxidase, involving NOX1, NOX2, and possibly NOX4.

Materials and Methods

Animal model

Hypertensive mice were generated by the infusion of Ang II into 10-week-old C57BL/6 mice and into *Nox1*-deficient mice with their control littermates as previously described (5). Briefly, an osmotic minipump (Alzet model 2002; Durect Corp., Cupertino, CA, USA) containing [Val⁵] Ang II (Sigma, St. Louis, MO, USA) or vehicle (phosphate-buffered saline: PBS) was inserted to permit the subcutaneous infusion of Ang II ($0.7 \text{ mg} \cdot \text{kg}^{-1} \cdot \text{day}^{-1}$) for 14 days. During the infusion period, atorvastatin ($20 \text{ mg} \cdot \text{kg}^{-1} \cdot \text{day}^{-1}$, p.o.) or vehicle (1.5% carboxymethylcellulose : 0.2% Tween-20, w/v) was administered.

For the model of atherosclerosis, 10-week-old apolipoprotein E (ApoE)-deficient and age-matched C57BL/6 mice were fed a high-fat, cholesterol-rich (HFCR; Oriental Yeast Co., Ltd., Tokyo) diet for 7 weeks. During the 7-week period, the same dose of atorvastatin was administered as described above.

The present study was performed with the approval of the Committee for Animal Research at Kyoto Prefectural University of Medicine.

Blood pressure measurements

Blood pressure in conscious mice was measured by the tail-cuff system using BP98A (Softron Co., Tokyo). Before the osmotic pump was implanted, at least 3 days of training were conducted to accustom mice to the procedure. For each time point, five measurements were obtained and averaged for each mouse.

Dihydroethidium (DHE) staining

The thoracic aorta was dissected and snap-frozen in liquid nitrogen after being embedded in Tissue-Tek O.C.T. compound (Sakura Finetechnical Co., Tokyo). Unfixed frozen ring segments were cut into 30- μm -thick sections and placed on a glass slide. DHE ($10 \mu\text{M}$; Molecular Probes, Eugene, OR, USA) was topically applied to each tissue section and coverslipped. Slides were incubated in a light-protected humidified chamber at 37°C for 30 min. For the detection of ethidium bromide, a 543-nm He-Ne laser combined with a 560-nm long-pass filter was used.

Detection of superoxide production

Superoxide production was measured by the lucigenin chemiluminescence method. Aortic rings (0.5 cm) were dissected and incubated for 30 min in Krebs-HEPES at 37°C . Rings were transferred to scintillation vials containing $5 \mu\text{M}$ lucigenin in Krebs-HEPES buffer and then incubated for 10 min at 37°C in the dark. After the incubation, chemiluminescence was measured by a luminometer (AB-220 Luminescencer PSN; ATTO Co., Tokyo) over 10 min at 1-min intervals. Following the measurement of the baseline chemiluminescence for 5 min, NADPH ($100 \mu\text{M}$) was added and data were taken for another 5 min. The lucigenin chemiluminescence was expressed as relative light units (RLU) per milligram of dry tissue weight per min.

Real-time PCR

The thoracic aorta of mice was dissected and snap-frozen in liquid nitrogen. Total RNA was isolated by the acid guanidinium thiocyanate/phenol/chloroform method. RNA was reverse-transcribed using the Superscript III First-Strand Synthesis System for RT-PCR (Invitrogen Corp., Carlsbad, CA, USA). Real-time PCR was performed using the 7300 Real Time PCR System (Applied Biosystems, Foster City, CA, USA) with the SYBR Premix Ex Taq (Takara Bio Inc., Shiga). Dissociation curves were monitored to check the aberrant formation of primer dimers. PCR-amplified products were electrophoresed on 2% agarose gels to confirm the presence of a single band. Copy numbers were calculated based on standard curves generated with genuine cDNA templates. The following sequence specific primers were used: Nox1, sense 5'-ctgacaagtac tattacacgagag-3', antisense 5'-catatatgccaccagcttatggaag-3'; Nox2, sense 5'-aactgtatgctgatcctgctgc-3', antisense 5'-gttctcattgtcaccgatgtcag-3'; Nox4, sense 5'-tgaggagtcact gaactatgaagttaac-3', antisense 5'-tgactgaggtacagctggatg ttcaca-3'.

Cell fractionation

The thoracic aorta of mice was dissected and snap-frozen in liquid nitrogen. Samples homogenized with lysis buffer containing 0.25 M sucrose and 5% protease inhibitor cocktail (Sigma) were centrifuged at $8,000 \times g$ for 10 min at 4°C . The supernatant was then centrifuged at $100,000 \times g$ for 30 min. The supernatant containing cytosolic proteins was collected. The pellet representing membrane proteins was resuspended in sample buffer (12 mM sodium deoxycholate, 3 mM SDS, and 1% Nonidet P40 in PBS containing 5% protease inhibitor) and supplied for immunoblotting.

Western blot analysis

Proteins were separated by SDS-PAGE and transferred to polyvinylidene difluoride membranes. After transfer, membranes were blocked with 5% nonfat milk and incubated overnight with an anti-Rac1 antibody (Upstate, Charlottesville, VA, USA) or with anti- β -actin antibody (Sigma). The membranes were incubated with horseradish peroxidase-conjugated secondary antibody before detection with ECL-Plus (GE Healthcare, Buckinghamshire, UK). The density of the band was analyzed using NIH Image J software (<http://rsbweb.nih.gov/ij/>).

Morphological analysis

Mice were anesthetized and transcardially perfused with 10 ml of PBS followed by 10 ml of 4% paraformaldehyde phosphate buffer under pressure (100 mmHg). The aorta placed in 4% formalin overnight was processed and embedded in paraffin. Three sections (6 μ m) were obtained from each descending thoracic aorta, 3-mm distal to the left subclavian artery at 500- μ m intervals and stained with Elastica Van Gieson stain (EVG). The medial areas were measured using Image J software.

To identify lipid deposits in the aorta, aortic tissue containing the arch and 1 cm of descending artery

measured from the left subclavian artery was excised. The positive areas were measured using Image J software following oil red staining (0.5%).

Statistics

Statistical analyses were performed with the Kruskal-Wallis test followed by the Dunnett test. For multiple treatment groups, a repeat-measure, two-way, or Latin-square design ANOVA followed by the Tukey-Kramer test was applied.

Results

Atorvastatin suppressed the elevation of blood pressure induced by Ang II-infusion

When atorvastatin was administered to mice infused with PBS, mean blood pressure (MBP) remained unchanged during the experimental period. In response to the continuous infusion of Ang II, MBP levels were similarly elevated in both the vehicle- and atorvastatin-treated groups until day 3 of treatment. From day 5 until day 14 of Ang II-infusion, however, the increase was significantly suppressed and a lower MBP was demonstrated in the atorvastatin-treated group compared with the vehicle-treated group (Fig. 1a).

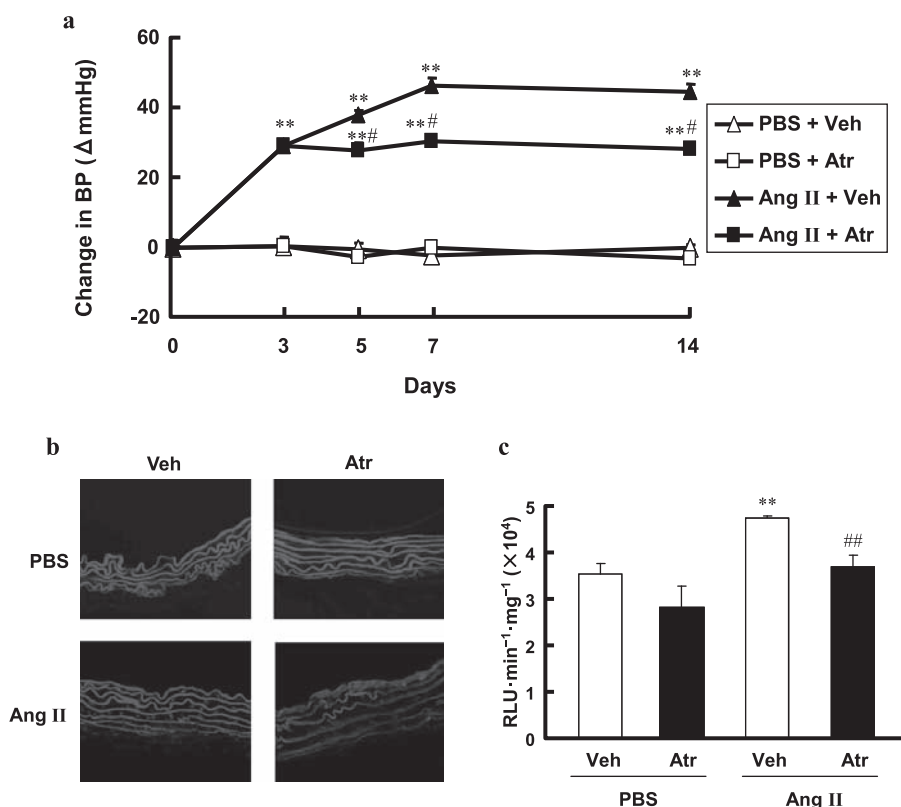


Fig. 1. Atorvastatin suppressed the elevation of blood pressure and superoxide production in the thoracic aorta of Ang II-infused mice. Atorvastatin (Atr) was administered to mice infused with Ang II or PBS. a) Mean blood pressure (MBP) was determined with the tail-cuff system as described in the Methods. Changes in blood pressure (BP) are shown based on the MBP on day 0. N = 6–9 per group. ** $P < 0.01$ vs. day 0, # $P < 0.05$ vs. corresponding vehicle-treated group (Veh). b) In situ detection of superoxide production with dihydroethidium (DHE). Cross sections of the thoracic aorta were obtained on day 14. Each image is representative of results from three animals. c) Levels of superoxide in the thoracic aorta were determined based on lucigenin chemiluminescence. N = 5–6 per group. ** $P < 0.01$ vs. corresponding PBS-infused group. # $P < 0.01$ vs. corresponding Veh.

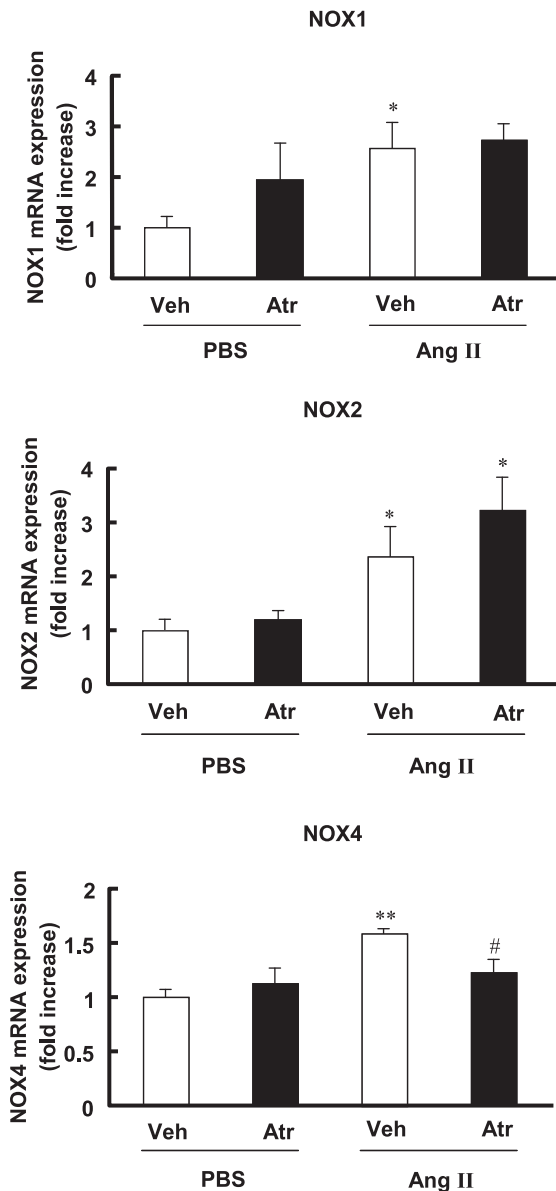


Fig. 2. Atorvastatin suppressed NOX4 mRNA expression induced by the infusion of Ang II. Total RNA was isolated from the thoracic aorta on day 14. NOX1, NOX2, and NOX4 mRNA levels were measured by real-time PCR. Data are shown as fold-increases relative to the control (PBS + Veh). N = 4–6 per group. * $P < 0.05$, ** $P < 0.01$ vs. corresponding PBS-infused group. # $P < 0.05$ vs. corresponding Veh.

Atorvastatin suppressed superoxide production in the thoracic aorta of Ang II-infused mice

To evaluate the effect of atorvastatin on vascular superoxide production, DHE staining was performed in the thoracic aorta of Ang II-infused mice (Fig. 1b). A low level of DHE fluorescence was detected in the thoracic aorta of both the vehicle- and atorvastatin-treated groups after the infusion of PBS for 14 days. DHE fluorescence in the aorta of vehicle-treated mice

was intensified after the infusion of Ang II for 14 days. On the other hand, DHE fluorescence was attenuated in the atorvastatin-treated group compared with the vehicle-treated group.

We next carried out the lucigenin chemiluminescence assay to ensure the effect of atorvastatin on vascular superoxide production. No difference in chemiluminescence was detected between the vehicle-treated and atorvastatin-treated groups infused with PBS. After the infusion of Ang II for 14 days, however, the chemiluminescence of the aorta was significantly less intense in the atorvastatin-treated group than the vehicle-treated group (Fig. 1c).

Atorvastatin reduced NOX4 mRNA expression in the thoracic aorta of Ang II-infused mice

Levels of NOX1, NOX2, and NOX4 mRNAs expressed in the thoracic aorta of PBS-infused control mice were 72.5 ± 15.8 , $(108.9 \pm 20.7) \times 10^3$, and $(3776.4 \pm 259.2) \times 10^3$ copies/ μg RNA, respectively. After Ang II-infusion for 14 days, levels of all NOX isoforms were significantly increased in the vehicle-treated group. Atorvastatin did not affect the mRNA levels of NOX1 and NOX2, whereas the level of NOX4 mRNA was significantly reduced in the Ang II-infused group (Fig. 2).

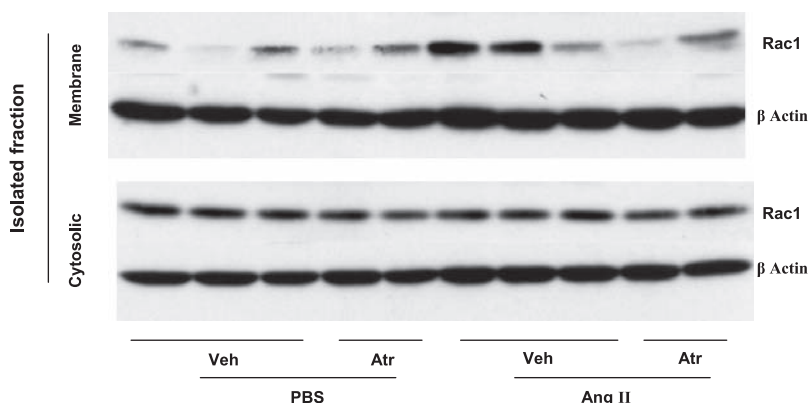
Atorvastatin reduced membrane translocation of Rac1 in the thoracic aorta of Ang II-infused mice

To verify the effect of atorvastatin on membrane translocation of Rac1, one of the cytosolic subunits necessary for the activation of NOX1 and NOX2/NADPH oxidases, we next examined the subcellular distribution of Rac1 in mice treated with atorvastatin. As shown in Fig. 3, a marked increase in the amount of Rac1 localized in the membrane fraction was observed in Ang II-infused mice. In the Ang II-infused group treated with atorvastatin, the membrane translocation of Rac1 was significantly suppressed. On the other hand, no significant difference in the amount of cytosolic Rac1 was detected among all groups. These results suggest that reduced translocation of Rac1 contributed to the anti-hypertensive effect of atorvastatin.

Atorvastatin did not affect Ang II-induced vascular hypertrophy

As vascular hypertrophy is closely linked to elevated blood pressure, we investigated the effect of atorvastatin on Ang II-induced vascular hypertrophy. When the medial area in cross-sections of the thoracic aorta was compared, the infusion of Ang II for 14 days was found to have induced significant hypertrophy in both the vehicle-treated and atorvastatin-treated groups. Thus the

a



b

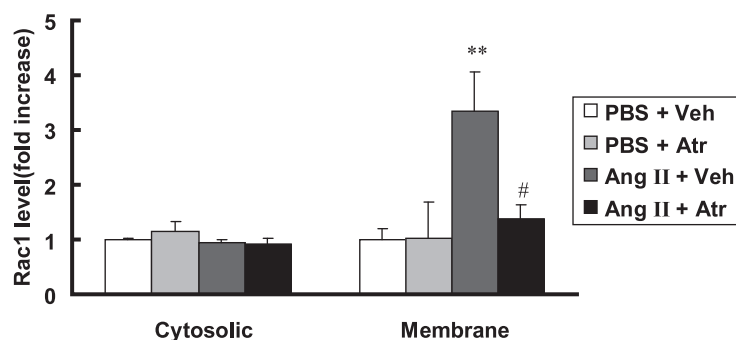


Fig. 3. Atorvastatin reduced membrane translocation of Rac1 in the thoracic aorta of Ang II-infused mice. a) Representative immunoblots of membrane and cytosolic fractions of aortic tissue. b) Quantitative densitometric analysis of Rac1 normalized by β -actin. Bars represent fold-increases relative to the control (PBS + Veh). N = 4–6 per group. ** $P < 0.01$ vs. corresponding PBS-infused group. # $P < 0.05$ vs. corresponding Veh.

administration of atorvastatin did not affect vascular remodeling induced by Ang II under our experimental conditions (Fig. 4).

Atorvastatin suppressed the elevation of blood pressure and decreased ROS production in ApoE-deficient mice

To better reproduce the setting for the clinical usage of statins, we examined the effects of atorvastatin on the blood pressure of ApoE-deficient mice on a high-fat diet. The administration of atorvastatin did not affect the MBP of wild-type mice during the experimental period. In ApoE-deficient mice fed a high-fat diet, MBP levels gradually elevated during 7 weeks. As shown in Fig. 5a, atorvastatin significantly suppressed the increase in MBP in ApoE-deficient mice.

When the effect of atorvastatin on vascular superoxide production was investigated, no difference was detected in the thoracic aorta of wild-type mice treated with statin. On the other hand, the marked increase in superoxide production demonstrated in ApoE-deficient mice was significantly attenuated in the group treated with atorvastatin (Fig. 5b).

Atorvastatin reduced the expression of NOX2 and NOX4 mRNAs in the thoracic aorta of ApoE-deficient mice

Next, levels of NOX mRNAs were investigated in

the thoracic aorta of ApoE-deficient mice fed a high-fat diet for 7 weeks. Levels of NOX1, NOX2, and NOX4 mRNAs expressed in the thoracic aorta of vehicle-treated wild-type mice were 113.1 ± 46.1 , $(32.1 \pm 6.4) \times 10^3$, and $(1008.4 \pm 212.3) \times 10^3$ copies/ μg RNA, respectively. As shown in Fig. 6, NOX2 and NOX4 mRNA levels were significantly increased in ApoE-deficient mice compared with wild-type mice. Both NOX2 and NOX4 mRNA levels in ApoE-deficient mice were significantly decreased by the treatment with atorvastatin during this period. No difference in the NOX1 mRNA level was detected among the experimental groups.

Atherosclerotic lesions in ApoE-deficient mice

To clarify whether the decreased blood pressure demonstrated in atorvastatin-treated mice was linked to the formation of atherosclerotic lesions, the size of atherosclerotic plaques in the aortic arch was determined by Oil-Red staining. The Oil-Red-positive area was significantly increased in ApoE-deficient mice compared with wild-type mice. With the dose of atorvastatin applied in this study, however, no statistically significant improvement in the oil-red-positive area was shown in ApoE-deficient mice treated with statin (Fig. 7: a and b). These findings suggest that the decreased MBP

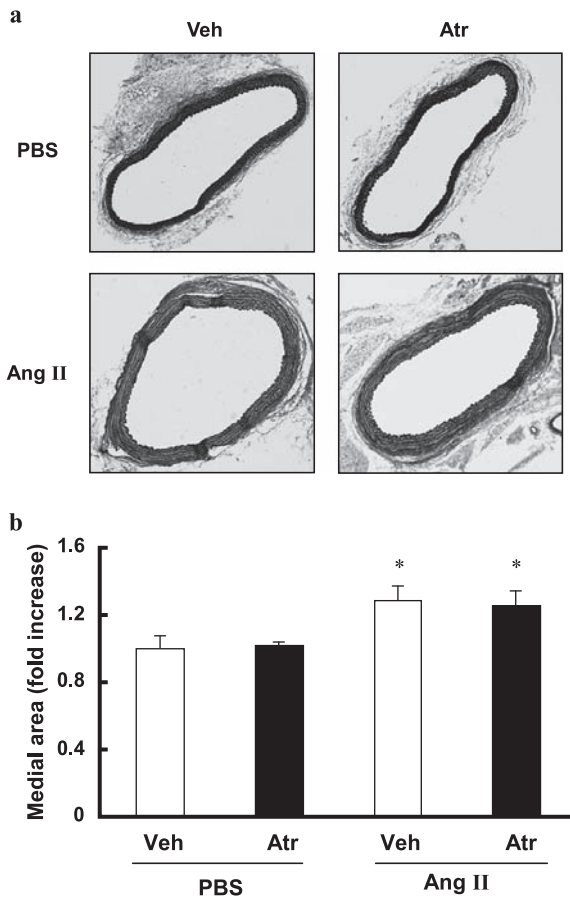


Fig. 4. Atorvastatin did not affect Ang II-induced vascular hypertrophy. a) Representative cross-sections of the thoracic aorta stained with Elastica Van Gieson stain. b) Quantitative analyses of the medial area. Ang II or PBS was infused for 14 days. N = 5 per group. * $P < 0.05$ vs. corresponding PBS-infused group.

demonstrated in atorvastatin-treated ApoE-deficient mice was not primarily related to the development of atherosclerotic lesions.

Atorvastatin reduced blood pressure in *Nox1*-deficient mice infused with Ang II

Finally, we examined the effect of atorvastatin on *Nox1*-deficient mice infused with Ang II. Our previous study indicated that NOX1 is involved in the late phase but not the early phase of the pressor response to Ang II (5). Consistent with our previous findings, the increase in MBP was significantly suppressed in *Nox1*-deficient mice on day 7 and 14 of Ang II-infusion. When atorvastatin was administered to wild-type mice infused with Ang II, the increase in MBP was suppressed compared with the vehicle-treated group. Notably, an additional decline in MBP was demonstrated when atorvastatin was administered to *Nox1*-deficient mice infused with Ang II (Fig. 8). These results suggest that the NOX

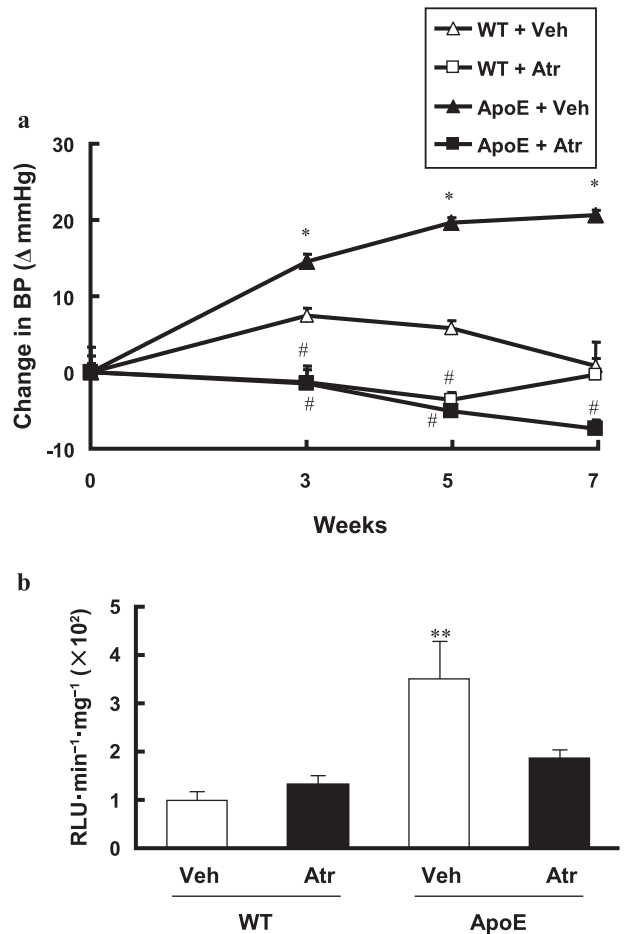


Fig. 5. Atorvastatin suppressed the elevation of blood pressure and decreased ROS production in ApoE-deficient mice. a) Changes in BP are shown based on MBP on day 0. N = 6 per group. * $P < 0.05$ vs. corresponding day 0. # $P < 0.05$ vs. corresponding Veh. b) Levels of superoxide in the thoracic aorta were determined based on lucigenin chemiluminescence. N = 5–6 per group. ** $P < 0.01$ vs. corresponding wild-type group (WT).

isoform other than NOX1 may also take part in the antihypertensive effects of atorvastatin.

Discussion

In this study, anti-hypertensive effects of atorvastatin were clearly demonstrated in Ang II-infused mice as well as in ApoE-deficient mice fed a high-fat diet. In both animal models, atorvastatin reduced ROS production and suppressed the expression of NOX4 mRNA in the aorta. In Ang II-infused mice, administration of atorvastatin decreased the translocation of Rac1 to the membrane fraction of aortic tissue. Interestingly, MBP was significantly decreased in Ang II-infused *Nox1*-deficient mice treated with atorvastatin. These findings suggest that atorvastatin exhibits antihypertensive effects possibly by reducing the expression and activity of

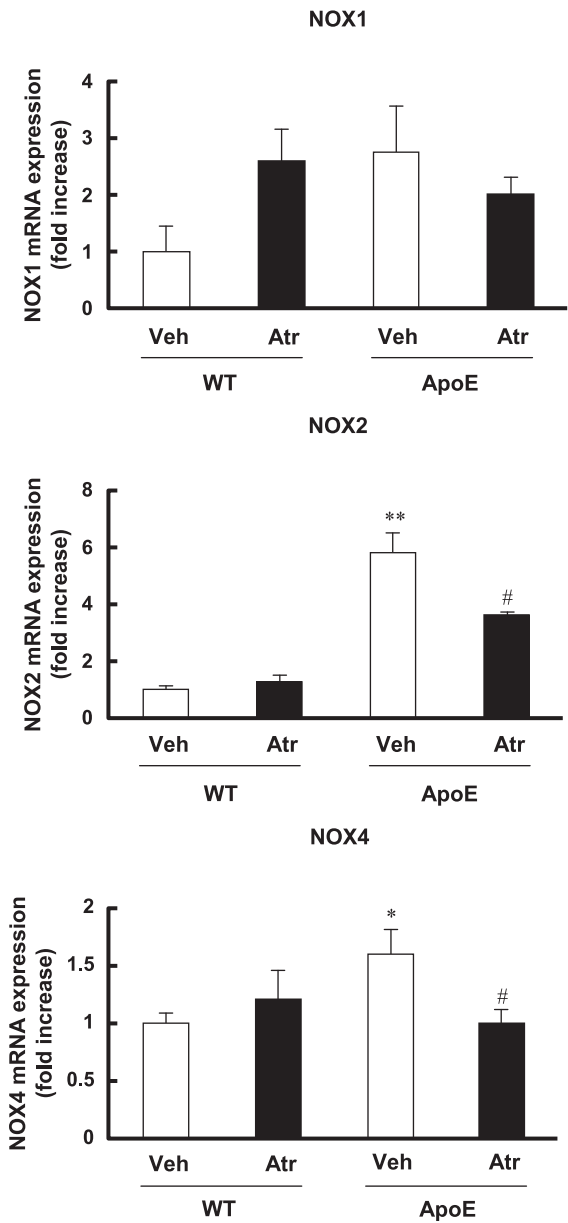


Fig. 6. Atorvastatin reduced expression of NOX2 and NOX4 mRNAs in ApoE-deficient mice. Total RNA was isolated from the thoracic aorta after 7 weeks on a high-fat diet. NOX1, NOX2, and NOX4 mRNA levels were measured by real-time PCR. Data are shown as fold-increases relative to the control (WT + Veh). N = 4 – 6 per group. * $P < 0.05$, ** $P < 0.01$ vs. corresponding WT. # $P < 0.05$ vs. corresponding Veh.

multiple NADPH oxidase isoforms.

Atorvastatin markedly attenuated the development of hypertension, and this effect was accompanied by reduced production of vascular ROS. Ang II, the main effector peptide of the renin–angiotensin system (RAS), plays a major role in the initiation and progression of hypertension, vascular hypertrophy, and atherosclerosis (14, 15). Various studies have demonstrated that ROS

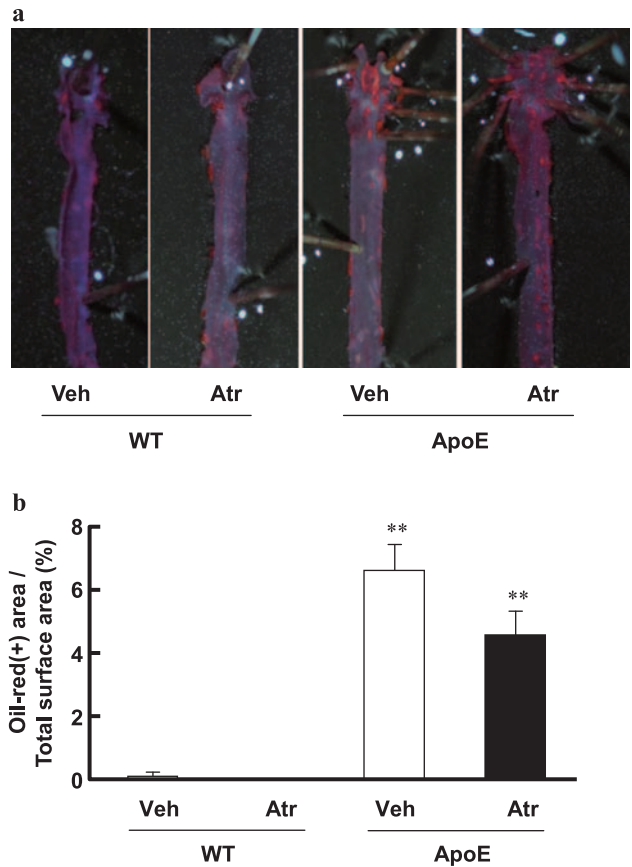


Fig. 7. Oil Red-positive area in ApoE-deficient mice. a) Representative aortic sections stained with Oil Red. b) Quantitative stereological analysis of Oil Red staining. N = 6 per group. ** $P < 0.01$ vs. corresponding WT.

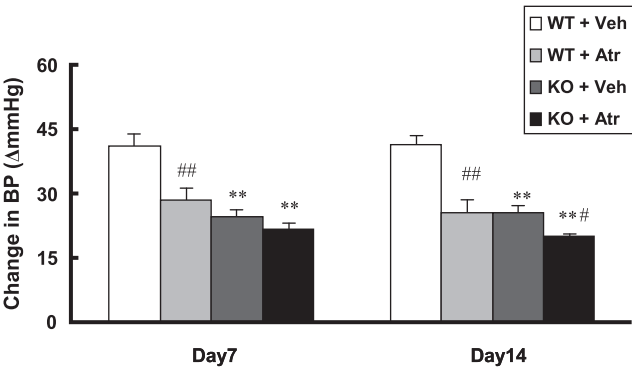


Fig. 8. Atorvastatin reduced blood pressure in Nox1-deficient mice infused with Ang II. Atorvastatin was administered to Nox1-deficient mice (KO) or wild-type littermates (WT) infused with Ang II. Changes in BP are shown based on the MBP on day 0 of Ang II-infusion. N = 6 per group. ** $P < 0.05$ vs. corresponding WT. * $P < 0.05$, ## $P < 0.01$ vs. corresponding Veh.

play an essential role in the development of hypertension by disrupting normal vasodilatory signaling pathways (5, 16). The decrease in blood pressure brought about by atorvastatin may be therefore attributed to the reduced generation of ROS in Ang II-induced hypertension. An increase in MBP was also observed in ApoE-deficient mice fed a high-fat diet, an animal model in which atherosclerotic lesions develop with an elevation of total cholesterol and triglyceride levels in plasma (17). Similar to the Ang II-infused model, atorvastatin blunted the elevation in blood pressure and suppressed ROS generation in ApoE-deficient mice. Since the increased blood pressure demonstrated in ApoE-deficient mice was associated with the development of atherosclerosis (18), there remains a possibility that the decrease in MBP was due to reduced atherosclerotic lesions in mice treated with atorvastatin. To test this possibility, the formation of atherosclerotic lesions was examined in the aorta of ApoE-deficient mice. In the present experimental conditions, however, treatment with atorvastatin did not significantly affect the development of atherosclerotic lesions, whereas it was sufficient to prevent the development of hypertension. These results indicated that the anti-hypertensive effect of atorvastatin on ApoE-deficient mice was not due to the improvement of atherosclerosis.

We presently demonstrated that treatment with atorvastatin down-regulated the expression of NOX4 mRNA in both animal models. In line with our findings, it was reported that treatment with pitavastatin suppressed vascular NOX4 expression in an animal model of congestive heart failure (19). However, to date, there is little information that supports the relationship between NOX4 and hypertension. In fact, the Ang II-induced increase in ROS production, which has been implicated in the pathogenesis of hypertension and vascular remodeling (4, 5), was not affected by depletion of NOX4 in aortic smooth muscle cells (20). Further research is needed to clarify the role of NOX4 in the development of hypertension.

Most of the beneficial effects of statins have been attributed to inhibition of Rac isoprenylation (21). Rac, a small GTPase, is required for the activity of NOX1 and NOX2/NADPH oxidase isoforms, but not NOX4 (22). Post-translational modification of Rac by isoprenylation is necessary for translocation to the plasma membrane, where it directly interacts with NOX1 or NOX2, followed by a subsequent interaction with a cytosolic activator subunit to generate ROS (23, 24). Translocation of Rac1 to the membrane fraction of aortic tissue was measured to verify the effect of atorvastatin on the activity of NADPH oxidase. Although mRNA levels of NOX1 and NOX2 were unchanged in our Ang II-infused model,

membrane translocation of Rac1 was significantly attenuated by the administration of atorvastatin. These findings were in line with the reduced generation of ROS demonstrated in the atorvastatin-treated group. The findings also endorse the concept that statins inhibit trafficking of Rac to disturb the assembly of the NADPH oxidase complex, thereby suppressing the activity of NADPH oxidase (25). Inhibition of Rac-dependent activation of NADPH oxidase may therefore underlie the anti-hypertensive effect of atorvastatin.

An additional decline in blood pressure was demonstrated when atorvastatin was administered to *Nox1*-deficient mice to characterize the NOX isoforms involved in the anti-hypertensive effect of statin. Thus the other NOX isoform of NADPH oxidase, NOX2, may take part in the anti-hypertensive effect of atorvastatin (26). On the other hand, it should be noted that the extent of the decline in MBP observed in *Nox1*-deficient mice treated with statin was less than the sum of the decline in wild-type mice treated with statin plus the decline in untreated knockout mice. Namely, there was no additive effect of atorvastatin and *Nox1* deficiency on Ang II-induced hypertension. If the effect of statin is NOX1-independent, the combined effect of atorvastatin and the abrogation of NOX1 would be additive. This fact, coupled with the findings in membrane translocation of Rac1 in aortic tissue, implies the involvement of both NOX1 and NOX2 in the antihypertensive effect of atorvastatin. As statins inhibit multiple molecules that are regulated by isoprenoids, there still remains the possibility that targets for statin other than NADPH oxidase also take part in the reduction in blood pressure observed in the present animal models.

In conclusion, atorvastatin suppressed increases in blood pressure in the Ang II-infused model as well as in ApoE-deficient mice fed a high-fat diet. The effect of atorvastatin is mediated by the Rac-dependent mechanism involving both NOX1 and NOX2/NADPH oxidases, and possibly reduced expression of NOX4.

References

- 1 Cakir Y, Ballinger SW. Reactive species-mediated regulation of cell signaling and the cell cycle: the role of MAPK. *Antioxid Redox Signal*. 2005;7:726–740.
- 2 Lambeth JD. Nox enzymes, ROS, and chronic disease: an example of antagonistic pleiotropy. *Free Radic Biol Med*. 2007;43:332–347.
- 3 Kakehi T, Yabe-Nishimura C. NOX enzymes and diabetic complications. *Semin Immunopathol*. 2008;30:301–314.
- 4 Bedard K, Krause KH. The NOX family of ROS-generating NADPH oxidases: physiology and pathophysiology. *Physiol Rev*. 2007;87:245–313.
- 5 Matsuno K, Yamada H, Iwata K, Jin D, Katsuyama M, Matsuki

- M, et al. Nox1 is involved in angiotensin II-mediated hypertension: a study in Nox1-deficient mice. *Circulation*. 2005;112:2677–2685.
- 6 Gavazzi G, Deffert C, Trocme C, Schappi M, Herrmann FR, Krause KH. NOX1 deficiency protects from aortic dissection in response to angiotensin II. *Hypertension*. 2007;50:189–196.
- 7 Lee MY, San Martin A, Mehta PK, Dikalova AE, Garrido AM, Datla SR, et al. Mechanisms of vascular smooth muscle NADPH oxidase 1 (Nox1) contribution to injury-induced neointimal formation. *Arterioscler Thromb Vasc Biol*. 2009;29:480–487.
- 8 Habibi J, Whaley-Connell A, Qazi MA, Hayden MR, Cooper SA, Tramontano A, et al. Rosuvastatin, a 3-hydroxy-3-methylglutaryl coenzyme a reductase inhibitor, decreases cardiac oxidative stress and remodeling in Ren2 transgenic rats. *Endocrinology*. 2007;148:2181–2188.
- 9 Tajima N, Kurata H, Nakaya N, Mizuno K, Ohashi Y, Kushiro T, et al. Pravastatin reduces the risk for cardiovascular disease in Japanese hypercholesterolemic patients with impaired fasting glucose or diabetes: diabetes subanalysis of the Management of Elevated Cholesterol in the Primary Prevention Group of Adult Japanese (MEGA) Study. *Atherosclerosis*. 2008;199:455–462.
- 10 Dechend R, Fiebeler A, Park JK, Muller DN, Theuer J, Mervaala E, et al. Amelioration of angiotensin II-induced cardiac injury by a 3-hydroxy-3-methylglutaryl coenzyme a reductase inhibitor. *Circulation*. 2001;104:576–581.
- 11 Sicard P, Delemasure S, Korandji C, Segueira-Le Grand A, Lauzier B, Guillard JC, et al. Anti-hypertensive effects of Rosuvastatin are associated with decreased inflammation and oxidative stress markers in hypertensive rats. *Free Radic Res*. 2008;42:226–236.
- 12 Wassmann S, Laufs U, Muller K, Konkol C, Ahlbory K, Baumer AT, et al. Cellular antioxidant effects of atorvastatin in vitro and in vivo. *Arterioscler Thromb Vasc Biol*. 2002;22:300–305.
- 13 Whaley-Connell A, Habibi J, Nistala R, Cooper SA, Karuparthi PR, Hayden MR, et al. Attenuation of NADPH oxidase activation and glomerular filtration barrier remodeling with statin treatment. *Hypertension*. 2008;51:474–480.
- 14 Kim S, Iwao H. Molecular and cellular mechanisms of angiotensin II-mediated cardiovascular and renal diseases. *Pharmacol Rev*. 2000;52:11–34.
- 15 Ferrario CM. Role of angiotensin II in cardiovascular disease therapeutic implications of more than a century of research. *J Renin Angiotensin Aldosterone Syst*. 2006;7:3–14.
- 16 Maron BA, Zhang YY, Handy DE, Beuve A, Tang SS, Loscalzo J, et al. Aldosterone increases oxidant stress to impair guanylyl cyclase activity by cysteinyl thiol oxidation in vascular smooth muscle cells. *J Biol Chem*. 2009;284:7665–7672.
- 17 Plump AS, Smith JD, Hayek T, Aalto-Setälä K, Walsh A, Verstuyft JG, et al. Severe hypercholesterolemia and atherosclerosis in apolipoprotein E-deficient mice created by homologous recombination in ES cells. *Cell*. 1992;71:343–353.
- 18 Yang R, Powell-Braxton L, Ogaoawara AK, Dybdal N, Bunting S, Ohneda O, et al. Hypertension and endothelial dysfunction in apolipoprotein E knockout mice. *Arterioscler Thromb Vasc Biol*. 1999;19:2762–2768.
- 19 Takayama T, Wada A, Tsutamoto T, Ohnishi M, Fujii M, Isono T, et al. Contribution of vascular NAD(P)H oxidase to endothelial dysfunction in heart failure and the therapeutic effects of HMG-CoA reductase inhibitor. *Circ J*. 2004;68:1067–1075.
- 20 Dikalov SI, Dikalova AE, Bikineyeva AT, Schmidt HH, Harrison DG, Griendling KK. Distinct roles of Nox1 and Nox4 in basal and angiotensin II-stimulated superoxide and hydrogen peroxide production. *Free Radic Biol Med*. 2008;45:1340–1351.
- 21 Takemoto M, Liao JK. Pleiotropic effects of 3-hydroxy-3-methylglutaryl coenzyme a reductase inhibitors. *Arterioscler Thromb Vasc Biol*. 2001;21:1712–1719.
- 22 Martyn KD, Frederick LM, von Loehneysen K, Dinanier MC, Knaus UG. Functional analysis of Nox4 reveals unique characteristics compared to other NADPH oxidases. *Cell Signal*. 2006;18:69–82.
- 23 Koga H, Terasawa H, Nunoi H, Takeshige K, Inagaki F, Sumimoto H. Tetratricopeptide repeat (TPR) motifs of p67(phox) participate in interaction with the small GTPase Rac and activation of the phagocyte NADPH oxidase. *J Biol Chem*. 1999;274:25051–25060.
- 24 Diebold BA, Bokoch GM. Molecular basis for Rac2 regulation of phagocyte NADPH oxidase. *Nat Immunol*. 2001;2:211–215.
- 25 Endres M, Laufs U. Effects of statins on endothelium and signaling mechanisms. *Stroke*. 2004;35:2708–2711.
- 26 Wang HD, Xu S, Johns DG, Du Y, Quinn MT, Cayatte AJ, et al. Role of NADPH oxidase in the vascular hypertrophic and oxidative stress response to angiotensin II in mice. *Circ Res*. 2001;88:947–953.